



Dempster, T.J., and Macdonald, F. (2016) Controls on fluid movement in crustal lithologies: evidence from zircon in metaconglomerates from Shetland. *Geofluids*, 16(3), pp. 507-517. (doi:[10.1111/gfl.12172](https://doi.org/10.1111/gfl.12172))

This is the author's final accepted version.

There may be differences between this version and the published version. You are advised to consult the publisher's version if you wish to cite from it.

<http://eprints.gla.ac.uk/117403/>

Deposited on: 10 March 2016

Enlighten – Research publications by members of the University of Glasgow
<http://eprints.gla.ac.uk>

Controls on fluid movement in crustal lithologies: evidence from zircon in metaconglomerates from Shetland

| | |
|-------------------------------|--|
| Journal: | <i>Geofluids</i> |
| Manuscript ID | GFL-2015-038.R2 |
| Manuscript Type: | Original Manuscript |
| Date Submitted by the Author: | n/a |
| Complete List of Authors: | Dempster, Tim; University of Glasgow, School of Geographical and Earth Sciences Macdonald, Fiona; University of Aberdeen, School of Geosciences |
| Key words: | zircon, fluids, deformation, permeability, metaconglomerate, quartzite, granite |
| | |

1
2
3 **Controls on fluid movement in crustal lithologies: evidence from zircon in**
4 **metaconglomerates from Shetland**
5
6
7

8
9 TIM DEMPSTER* & FIONA MACDONALD¹
10

11 *School of Geographical and Earth Sciences, University of Glasgow, Glasgow G12*
12 *8QQ, UK.*
13
14
15

16
17
18 Running title: Monitoring permeability in crustal rocks using zircon textures
19

20 Key words: zircon, fluids, permeability, deformation, conglomerate
21
22

23
24
25 * Corresponding author: T.J. Dempster, School of Geographical and Earth
26 Sciences, University of Glasgow, Glasgow G12 8QQ, UK.
27
28

29 Tel: +44 (0) 1413305445
30

31 Fax: +44 (0) 1413304817
32

33 Email: Tim.Dempster@glasgow.ac.uk
34
35
36
37

38 1. Present address: School of Geosciences, University of Aberdeen, Old
39 Aberdeen AB24 3UE, UK.
40
41
42
43
44
45
46
47
48
49
50
51
52
53
54
55
56
57
58
59
60

ABSTRACT

An investigation of the morphology of zircon in clasts and matrix of a greenschist facies metaconglomerate from Shetland has revealed a history of alteration of radiation-damaged grains, partial dissolution and growth of new zircon. These processes are linked to the generation of chemically modified dark BSE zircon that is spatially related to fractures generated during radiation damage; embayments and rounding of zircon margins; and late overgrowths of original grains. These late modifications of zircon are all linked to the presence of fluids and so zircon morphology is used to track fluid behaviour in different lithologies in the metaconglomerate. Alteration is unrelated to clast margins and radically different in various clast types. This reflects a difference in permeability and suggests that deformation strongly controls fluid influx into quartzite, whereas zircon alteration in granite is associated with a restricted permeability reflecting the more limited response to deformation events.

INTRODUCTION

Fluids in the Earth's crust are important in many respects; they may control mineral reactions, influence deformation processes, facilitate heat transfer and the accumulation of economic resources (Ferry 1984; Bickle & McKenzie 1987; Chamberlain & Rumble 1988; Yardley 2009). The movement of fluids in deep crustal rocks is typically monitored by chemical or isotopic techniques through the analysis of minerals thought to have been in equilibrium with those fluids (Kohn & Valley 1994; Skelton *et al.* 1995; Cartwright 1997; Pitcairn *et al.* 2010). Fluid pathways may be constrained by textural evidence of localized mineral dissolution and new growth (Holness & Watt 2001; Oliver & Bons 2001; Dempster *et al.* 2006). Thus reactive and

1
2
3 soluble phases may be dissolved in one location, components transported within the
4 fluid and re-precipitated in a distal site where conditions are sufficiently different to
5 promote crystallization.
6
7

8
9
10 Zircon is present in many common crustal rock types (Harley & Kelly 2007) and has
11 the advantage in regards to monitoring fluid interactions in that in some forms it is
12 very stable (Wilde *et al.* 2001, Kröner, 2010); but in a radiation-damaged state it is
13 exceptionally reactive and prone to alteration in the presence of fluids (Dempster *et*
14 *al.* 2004; Ramussen 2005; Hay & Dempster 2009a,b). In this damaged and altered
15 state zircon commonly experiences dissolution in hydrous fluids (Ewing *et al.* 1982;
16 Delattre *et al.* 2007; Geisler *et al.* 2007). Local re-precipitation of that reactive zircon
17 in a stable form is favoured by the generally low capacity of hydrous fluids to
18 incorporate high Zr concentrations (e.g. Ayers & Watson 1991). As a consequence,
19 evidence of both dissolution and reprecipitation are typically observed in adjacent
20 areas or within the same crystal. Hence zircon textures can provide information on
21 initial fluid access and scales of fluid migration (Dempster *et al.* 2008b; Dempster &
22 Chung 2013).
23
24
25
26
27
28
29
30
31
32
33
34
35
36
37

38 In this study we use variations in the morphology of zircon within and between
39 adjacent clasts and matrix to assess controls on fluid movements within
40 metaconglomerates from the island of Fetlar, northeast Shetland, UK.
41
42

43 Metaconglomerates represent a potentially useful rock type to assess lithological
44 controls on fluid distribution as adjacent clasts and matrix may share a common
45 metamorphic history. As such metaconglomerates may represent an ideal test site for
46 variety of petrological processes.
47
48
49
50
51
52
53
54
55

56 **GEOLOGICAL SETTING AND PETROGRAPHY**

57
58
59
60

1
2
3 Samples were collected from two coastal sites on Funzie Ness, in the southeast of
4 Fetlar, Shetland at locations HU65476 88658 and HU66370 89523 (UK Ordnance
5 Survey Grid). The metaconglomerates mapped and documented by Flinn (1956),
6
7 contain abundant clasts of quartzite, with rarer marble, granite and schist. Clast sizes
8
9 are typically 10-20 cm long and have been deformed during regional metamorphism
10
11 such that they are both flattened and elongated within a fine grained phyllite matrix
12
13 (Fig.1). Clasts typically form >50% of the metaconglomerate throughout the outcrop
14
15 area. The external fabric anastomoses around the clasts and “pressure shadow”
16
17 triangular areas are present at the ends of the larger clasts containing fine grained
18
19 quartz (Fig. 2A). The timing of deformation is uncertain but style of deformation
20
21 varies slightly with proximity to the faulted contact with the Caledonian Unst
22
23 ophiolite to the west (Flinn 1956; Flinn & Oglethorpe 2005; Crowley & Strachan
24
25 2015). Although the metamorphic grade of the metaconglomerate matrix appears to
26
27 be identical at both sample sites, overall deformation intensity is slightly lower
28
29 towards the southwest of the area, at sample site HU65476 88658, with marginally
30
31 greater elongation of clasts but less constriction (Flinn 1956).
32
33 Quartzite clasts are dominated by >98% quartz with minor amounts of muscovite
34
35 (Fig. 2B), biotite, plagioclase, epidote and zircon. Quartz (up to 500 μm by 300 μm)
36
37 typically shows a well-developed shape fabric (Fig. 2B,C), with bulging
38
39 recrystallization on the grain boundaries of larger crystals which show subgrain
40
41 formation. Phyllosilicates are aligned along thin discontinuous anastomosing bands
42
43 that are parallel to the fabric in the matrix (Fig. 2A). Some variation in the intensity of
44
45 deformation is shown by the internal shape fabric of the clasts and correlates with
46
47 average grain size of the quartz (Fig. 2B,C). Muscovite is typically fine grained but
48
49 individual flakes may occur up to 500 μm (Fig. 2B). Biotite is relatively sparse and
50
51
52
53
54
55
56
57
58
59
60

1
2
3 typically unevenly distributed within the quartzite clasts with greater concentrations
4
5 around the edge of the clast. Locally biotite shows minor alteration to chlorite. Quartz
6
7 fabrics in the clasts are consistently aligned between individual clasts and sub-parallel
8
9 to the external fabric in the matrix. Deformation as shown by the quartz fabric may be
10
11 locally more intense near the edge of the clasts. The clasts show a sharp well defined
12
13 boundaries with the matrix marked by the consistently coarser grain size of quartz in
14
15 the former (Fig. 2A)..

16
17
18 Granite clasts are also elongate and slightly flattened, but typically smaller and less
19
20 obviously strained than those of quartzite. In the unaltered parts of the clasts they
21
22 contain abundant plagioclase (50%) and quartz (45%) (Fig. 2G,H), together with
23
24 muscovite and trace amounts of biotite. Fabrics with weak alignment parallel to the
25
26 foliation of the matrix are present within localised areas of finer grained quartz (Fig.
27
28 2H) but are not as strongly developed as within the quartzite clasts. Large (1-2 mm)
29
30 plagioclase shows less evidence of deformation and may show relict subhedral shapes
31
32 within a typically recrystallised finer grained quartz matrix (Fig. 2G) in a possible
33
34 relict interstitial texture. Clusters of coarser grained (100-200 μm) muscovite typically
35
36 lack alignment. Plagioclase shows patchy alteration within the granite, from sparse
37
38 sericitization to almost complete alteration to very fine grained phyllosilicates (Fig.
39
40 2F). Areas showing the latter may have a slightly more intense fabric with aligned
41
42 muscovite and biotite. Even at the very edge of granite clasts (Fig. 2F), the fabric
43
44 within the phyllosilicates is not strongly developed.

45
46
47 The matrix of the metaconglomerate contains mm-thick layers with abundant strongly
48
49 aligned muscovite and locally biotite and epidote (Fig. 2E). These are interbanded
50
51 with more quartz-rich layers, some of which may represent highly attenuated small
52
53 clasts and some original quartz-rich beds (Fig. 2D). Muscovite in the phyllitic layers
54
55
56
57
58
59
60

1
2
3 is typically fine grained (50-200 μm) although sparse larger 2 mm grains are present
4
5 and these may show evidence of late kinking (Fig. 2E). Clasts of individual quartz and
6
7 plagioclase grains and lithic clasts of granular quartzo-feldspathic rock within the
8
9 matrix typically have a strong shape fabric (Fig. 2E), with beards of white mica and
10
11 local pressure shadows adjacent to the large clasts. The larger individual grains are
12
13 approximately 0.5 - 1 mm diameter. Biotite tends to occur both within aligned clusters
14
15 and sparse larger books with cleavage oriented at high angles to the rock fabric (Fig.
16
17 2F). Locally very fine grained mylonitic layers occur parallel to the fabric in the
18
19 matrix (Fig. 2D). These layers are ca. 2 mm thick with isolated small ($<50 \mu\text{m}$)
20
21 porphyroclasts of quartz in a muscovite- and epidote-rich matrix.
22
23

24
25 The presence of matrix biotite, the grain size of the fabric forming muscovite, and the
26
27 quartz grain boundary textures, all indicate that the metaconglomerate has
28
29 experienced greenschist facies regional metamorphism. Strain is generally
30
31 homogeneous through the bulk of the rock but also localized in some thin mylonitic
32
33 zones within the matrix. Fabrics are typically parallel in the matrix and clasts,
34
35 although some refraction at the edges of the clasts is also present. The quartzite clasts
36
37 have experienced an earlier metamorphism, as evidenced by their larger grain size of
38
39 than the matrix and the sharp nature of the clast boundaries. However there is no
40
41 evidence of any pre-existing alignment associated with that earlier event.
42
43
44
45
46

47 **METHODS**

48
49 Zircon morphology was characterized using a FEI Quanta 200F field-emission
50
51 environmental scanning electron microscope at the University of Glasgow operated at
52
53 20 kV on polished thin sections of each sample. A total of five polished sections from
54
55 representative clasts were characterized with each section containing a matrix/clast
56
57
58
59
60

1
2
3 boundary; two polished sections were from granite clasts from sample site HU66370
4
5 89523 and three from quartzite clasts from locality HU65476 88658. Thin section
6
7 petrography of clasts from both sites confirms that those selected are representative.
8
9 Textural characterization of zircon was achieved through X-ray mapping to locate all
10
11 zircon grains in each thin section and backscattered electron (BSE) imaging of the
12
13 individual grains and adjacent matrix phases.
14
15
16
17

18 RESULTS

20 Zircon characteristics

21
22 Zircon is particularly abundant within the matrix but also common in both the
23
24 quartzite and granite clasts. Typically zircon is small with a 5-6 μm average radius
25
26 (Figs 3 & 4), and a maximum radius of ca. 50 μm is observed. Although rare small ca.
27
28 1 μm radius zircons are present, no micro-zircon (cf. Dempster *et al.* 2008a) are
29
30 present in any of the lithologies examined. Most zircons are equant, and some are
31
32 euhedral, although zircons in both the quartzite and matrix are characterized by a
33
34 slightly more rounded appearance than those in the granite clast. About 10% of all
35
36 zircons show evidence of brittle deformation (Fig. 3A), typically with fragments of
37
38 the original grain being displaced and dispersed parallel to cleavage in both the
39
40 quartzite clast (Fig. 3G) and the matrix (Fig. 4F,H,I). Zircon is characterized by a
41
42 range of alteration textures which may affect the whole grain or be confined to
43
44 original concentric growth zones (Figs 3 & 4). Radial cracks are commonly present
45
46 within the zircon (Fig. 4B). Alteration may produce different types, either a dark
47
48 heterogeneous texture in BSE images (Hay & Dempster 2009a) or a more uniform
49
50 alteration (Geisler *et al.* 2003; Rayner *et al.* 2005; Geisler *et al.* 2007; Hay &
51
52 Dempster 2009b). Both types of alteration may be spatially linked to radial cracks
53
54
55
56
57
58
59
60

1
2
3 within the original host zircon (Figs 3F,4B). The heterogeneous altered zircon has a
4 porous structure with a patchy inclusion-rich appearance (Fig 3D,G). Zircons showing
5 this type of alteration are commonly completely altered and altered areas of the zircon
6 are typically in contact with surrounding minerals. The more homogeneous type of
7 altered dark BSE zircon contains randomly oriented cracks (Fig. 4C), it may replace
8 large areas of the original host or may be confined to particular growth zones (Fig.
9 3B) and may also form bulbous structures within the host (Fig. 3A). Such altered
10 zircons typically retain their original shape (Fig. 4A) better than those with the
11 heterogeneous alteration (Fig. 4I). Highly porous light BSE zircon is also present
12 (Fig. 3H), and is most abundant in the quartzite clasts. About 10% of the whole zircon
13 population contains no dark BSE zircon and are apparently chemically unaltered
14 (Figs. 3E,4D). Small overgrowths of either light or dark BSE zircon may also be
15 present along the margins of some host zircons forming either isolated tiny (<1 μm)
16 pyramidal protrusions from the grain surface (Fig. 3H) or a thicker semi-continuous
17 crust around existing grains (Fig. 3C). In some instances, such overgrowths may also
18 form on fractured surfaces of the host grain. Rare xenotime is present as overgrowths
19 on altered zircon within the quartzite (Fig. 3D). Hence the rocks contain the same low
20 temperature zircon assemblages that Hay and Dempster (2009a,b) have reported from
21 both slates and sandstones.
22
23
24
25
26
27
28
29
30
31
32
33
34
35
36
37
38
39
40
41
42
43
44
45
46
47

48 **Characteristics of zircon in the granite clasts**

49 A total of 145 zircons were characterized in granite clasts. Generally less zircon is
50 present in the areas with coarse grained feldspars and may reflect an original feature
51 of the granite. Relatively unaltered zircon is more evenly distributed on the scale of a
52 thin section, and the distribution of the highly altered zircon is more clustered.
53
54
55
56
57
58
59
60

1
2
3 Despite these differences there are many instances where unaltered zircon occurs in
4 close proximity to highly altered zircon. The zircons are typically equant, euhedral
5 and overgrowths are only rarely developed (Fig. 5) and when present typically very
6 small ($<1 \mu\text{m}$). Alteration to dark BSE zircon rarely affects the whole grain and is
7 typically restricted to particular growth zones of the zircon, often in internal areas
8 (Fig. 3B). Some zircons show alteration confined to particular growth zones but
9 alteration fronts may be unrelated to the geometry of those growth zones (Fig. 3A).
10 The proportion of zircon in the granite that lacks any alteration is low (Fig. 6) and the
11 average amount of alteration in the zircon in the granite clast is high. Higher
12 proportions of altered zircon occur next to quartz and plagioclase than adjacent to
13 muscovite. Alteration typically produces homogeneous dark BSE zircon, with only
14 4% of the zircons showing exclusively heterogeneous alteration (Fig. 7). No porous
15 light BSE zircon is present in the granite clast. 8% of the zircons in the granite show
16 evidence of deformation. The alteration of zircon shows no systematic relationship to
17 proximity to the edge of the clast (Fig. 8).
18
19
20
21
22
23
24
25
26
27
28
29
30
31
32
33
34
35
36
37
38

39 **Characteristics of zircon in the quartzite clasts**

40 A total of 175 zircons were characterized in the quartzite clasts. The quartzite contains
41 generally equant slightly rounded zircons. A few euhedral grains are present and these
42 are typically small unaltered and enclosed within single grains of quartz (Fig. 3E).
43
44
45
46

47 Complex overgrowths are present on some zircons (Fig. 3C). Many grains with high
48 degrees of dark BSE alteration are present (Fig. 6) and these typically have irregular
49 margins (Fig. 3D, G). The quartzite clasts contain high proportions of the most altered
50 zircon but also high proportions of virtually unaltered zircon (Fig. 6). The alteration
51 of zircon and the abundance of overgrowths in the quartzite clasts are independent of
52
53
54
55
56
57
58
59
60

1
2
3 the proximity to the clast edge (Fig. 8). Heterogeneous dark BSE alteration is
4
5 dominant (Fig. 7) and porous light BSE zircon (Fig. 3H) is also relatively abundant.
6
7 Radial fractures are common within zircon even in those lacking dark BSE zircon.
8
9 14% of zircons show evidence of break-up and brittle deformation, this is particularly
10
11 associated with some of the most highly altered zircon (Fig. 3G). Typically fracturing
12
13 is associated with minor displacements and quartz infills the fractures. Overgrowths
14
15 are larger and higher proportions of alteration occur adjacent to muscovite than
16
17 adjacent to quartz (Fig. 8). Given the relative paucity of micas within the quartzite
18
19 clasts (<1%) a high proportion of zircons (ca. 40%) are adjacent to phyllosilicates.
20
21 19% of zircons contain a proportion of porous structure (Fig. 7) and 82% of these are
22
23 adjacent to quartz. Porous zircon rarely occurs next to muscovite and those that do are
24
25 typically partly altered to heterogeneous dark BSE zircon (Fig. 3G).
26
27
28
29
30
31

32 **Characteristics of zircon in the metaconglomerate matrix**

33
34 A total of 516 zircons were examined from the matrix. These are from a range of
35
36 different textural sites, including: the phyllosilicate-rich phyllite layers; a thin
37
38 mylonite; quartz-rich layers; and, quartz-rich patches within the “pressure shadow”
39
40 areas at the ends of elongate clasts. Zircons in the matrix are of similar size to those in
41
42 clasts. 18% of zircons in the matrix show evidence of deformation and displacement
43
44 along fractures, with grains broken up and dispersed along the line of the cleavage
45
46 (Fig. 4F). Such fractured zircon typically has subrounded crystal edges and there is a
47
48 lack of small angular fragments associated with the brittle deformation (Fig. 4H,J). A
49
50 few small euhedral zircon are present (Fig. 4D). Overgrowths are both large and
51
52 abundant on zircon in the matrix (Fig. 4E,G). The mylonite bands within the matrix
53
54 contain the highest proportions of zircon overgrowths (Fig. 5). Altered grains are
55
56
57
58
59
60

1
2
3 abundant but overall proportions of alteration are relatively low and 60% of zircon
4
5 grains show <10% alteration (Fig. 6). Alteration and the formation of overgrowths are
6
7 both more common in zircons adjacent to phyllosilicates rather than quartz (Fig. 9).
8
9 Heterogeneous alteration very commonly occurs in zircon next to muscovite and such
10
11 zircon also shows most evidence of deformation. Porous zircon is uncommon in the
12
13 matrix (Fig. 7). Homogeneous alteration of zircon is dominant in the matrix (Fig. 7)
14
15 and such alteration is most frequently confined within cores or growth zones. As such
16
17 these zircons tend to have more euhedral forms. Dark homogeneous BSE zircon that
18
19 is within the internal parts of the grain is linked to fluid access along radial cracks in
20
21 the outer parts of the grain (Fig. 4B). Those grains showing heterogeneous alteration
22
23 typically have very irregular margins, and frequently have major embayments and
24
25 show partial replacement by quartz (Fig. 4I).
26
27
28
29
30
31

32 **Variations between clasts and matrix and between different clast types**

33
34 Typically less alteration is observed in the matrix zircons, which are characterized by
35
36 few grains with very high proportions of alteration and many with no evidence of
37
38 alteration (Fig. 6). The matrix zircons also show the most evidence of deformation
39
40 and the textures of both altered and fractured grains indicate that significant
41
42 dissolution of both altered and unaltered zircon has occurred. Overgrowths are both
43
44 more abundant and larger on zircons in the matrix than those in either clast type (Fig.
45
46 5). Homogeneous alteration is dominant in the matrix zircon and very few porous
47
48 zircons are present (Fig. 7). Both alteration and new growth of zircon appears to be
49
50 favoured by proximity to muscovite (Fig. 9).
51
52

53
54 The largest differences between zircon types present are those between zircons in the
55
56 granite and quartzite clasts. Those within quartzite are characterized by intermediate
57
58
59
60

1
2
3 proportions of altered zircon, but abundant highly altered grains, and relatively rare
4 overgrowths. Alteration is dominated by heterogeneous grains, and, relative to other
5 parts of the metaconglomerate, chemically unmodified porous zircon is abundant (Fig.
6
7
8 7). Given the overall low proportion of muscovite present within the quartzite clasts
9
10 many zircons are adjacent to muscovite grains. Those zircons adjacent to muscovite
11
12 within the quartzite, are much more likely to have overgrowths and show alteration
13
14 (Fig. 9). In contrast to the other forms of alteration, a far lower proportion of porous
15
16 zircon occurs adjacent to muscovite.
17
18
19

20
21 The granite clast is dominated by homogeneous alteration of zircon, and no porous
22
23 zircon is present (Fig. 7). Although the average amount of alteration is highest within
24
25 the granite clast, very few zircons are completely altered, very few are completely
26
27 unaltered (Fig. 6) and very few overgrowths are present (Fig. 5). The parts of the
28
29 granite clast with more sericitization of plagioclase typically contain slightly less
30
31 altered zircon and may have fewer overgrowths.
32
33
34
35

36 INTERPRETATION

37 Zircon Textures

38
39 The interpretation of the textures of zircon follows earlier publications on low
40
41 temperature zircon morphology (e.g. Hay & Dempster 2009a):
42
43

44
45 *Light BSE zircon* represents chemically unmodified zircon (e.g. Fig 3E).
46

47
48 *Fractured zircon* occurs in two types: Radial or less commonly concentric fractures
49
50 that are spatially linked to growth zones in the host grain are associated with volume
51
52 changes in the lattice of the zircon due to radiation damage (Lee & Tromp 1995) (e.g.
53
54 Fig. 4B). Fractures with large displacements are unrelated to internal zoning structure
55
56 of the zircon and are associated with deformation events (e.g. Fig. 4J).
57
58
59
60

1
2
3 *Porous zircon* has a modified structure but a light BSE signature that indicates a lack
4 of chemical change. These are interpreted as recovery of zircon from a metamict state
5 that have been isolated from fluids. Evidence for radiation damage having caused the
6 structural modification is manifested by radiation related fractures (e.g. Fig. 3H).

7
8
9
10
11 *Overgrowths* of newly formed zircon that may have little relationship to the structural
12 state of the host grain (e.g. Fig. 3C) suggests significant redistribution of Zr and
13 mobility within a fluid phase.
14
15

16
17
18 *Embayment of zircon* margins and rounding of the edges of fragments implies
19 dissolution of the host grain. This is most obvious where deformation related
20 fracturing has occurred and there is an absence of angular edges or small fragments of
21 zircon (e.g. Fig. 4I).
22
23

24
25
26
27 *Dark BSE zircon* is chemically modified and represents fluid access to structurally
28 modified grains. Typically evidence of fluid access along radiation damage-related
29 fractures is observed. Alteration occurs in two distinct forms:
30
31

32
33
34 *Heterogeneous altered zircon* is thought to form through a dissolution and
35 reprecipitation mechanism (Geisler *et al.* 2007) in a high permeability environment
36 with ready access to fluids. Such zircon is known to have a nanocrystalline structure
37 and is most typically found in low-grade metamorphic environments (Hay &
38 Dempster 2009a). Porous zircon and heterogeneous altered zircon, which itself has a
39 porous structure, are frequently observed within the same grain suggesting that the
40 former alter to produce the latter (e.g. Fig. 3G).
41
42
43
44
45
46
47
48

49
50 *Homogeneous altered zircon* may form as a result of in-situ diffusion driven
51 structural recovery (Geisler *et al.* 2004; 2007). Although this recrystallisation must
52 occur in the presence of fluid, it represents more of a closed system with restricted
53 access to fluid and hence a lower permeability and higher levels of Zr saturation in the
54
55
56
57
58
59
60

1
2
3 fluid. It is known to have a microcrystalline structure (Hay & Dempster 2009b)
4
5 lacking inclusions and it is notable that this type of alteration is often restricted to
6
7 internal zones or patches within the host grain (e.g. Fig. 3B) and as such may be less
8
9 prone to subsequent dissolution than the heterogeneous altered forms. Such altered
10
11 zircon has previously been observed to form in low temperature sedimentary
12
13 environments (Hay & Dempster 2009b).
14
15
16
17

18 **Timing of Zircon Alteration**

20
21 Many of the alteration and overgrowth characteristics of zircon in both the quartzite
22
23 and matrix are influenced by the adjacent mineralogy (Fig. 9). This spatial association
24
25 is controlled by the in-situ deformation and metamorphic conditions. Hence the
26
27 timing of much of the zircon alteration and formation of any overgrowths is either
28
29 associated with, or post-dates, the metamorphic event. The evidence from the grain
30
31 size of the quartzite clasts suggests that they were initially quartzite, not sandstone
32
33 clasts. However the flattening of the clasts themselves and the mineral alignment
34
35 within the clasts appears to be entirely related to the deformation of the conglomerate.
36
37 There is no evidence of an earlier deformation event in the clasts. The relationship
38
39 between zircon alteration and deformation is less clear-cut in the granite clasts due to
40
41 the lack of a consistent penetrative metamorphic fabric. The presence of similar
42
43 zircon alteration textures in the granite clast to those in the matrix suggests that most
44
45 of the alteration of zircon in the granite may also post-date the sedimentary history of
46
47 the clast. The nature of the alteration to zircon in all the lithologies that have been
48
49 studied is also compatible with greenschist facies metamorphism of the conglomerate
50
51 (Hay & Dempster 2009a).
52
53
54
55
56
57
58
59
60

1
2
3 The zircon population in the matrix may come from a variety of different sources,
4
5 some may represent disaggregated quartzite and granite and some from other sources,
6
7 although the abundance of zircon does not suggest a major contribution from
8
9 ophiolitic material (*cf.* Flinn & Oglethorpe 2005). The generally rounded shape of the
10
11 relatively unaltered zircon in the matrix is compatible with a detrital origin and those
12
13 in a highly altered state would be unlikely to survive transportation in a high energy
14
15 sedimentary environment. This also suggests that any subsequent alteration of zircon
16
17 within the matrix that is linked to the build up of radiation damage is likely to
18
19 significantly post-date the sedimentary history. Consequently although there is
20
21 uncertainty as to the exact timing of zircon alteration it is thought likely that a high
22
23 proportion of the alteration occurred during the later stages of the evolution of the
24
25 metaconglomerate rather than early sedimentary processes.
26
27

28
29 Initial zircon populations in the various clasts and matrix may be different. However,
30
31 virtually all of the zircons irrespective of their location in the rocks are prone to
32
33 subsequent alteration. Many of those that show no chemical modification typically do
34
35 show either a porous structure or contain radiation-damage related cracks (Lee &
36
37 Tromp 1995) that suggest they have experienced structural modification. As such it is
38
39 suggested that the only reason that some zircons show little or no chemical
40
41 modification is due to a lack of interaction with fluids. Given that zircons with both
42
43 types of alteration are present in overall similar proportions, the alteration type is
44
45 unlikely to be controlled by temperature (*cf.* Hay & Dempster 2009b). The metamict
46
47 state of the original grain is also not a dominant control (Hay & Dempster 2009b) but
48
49 the alteration type is a reflection of the differing response to fluid access.
50
51

52
53 Consequently the presence or absence of chemical alteration and indeed the type of
54
55 alteration are all potential proxies for monitoring fluid pathways or local fluid
56
57
58
59
60

1
2
3 composition. Although the latter is known to control zircon solubility (Ayers *et al.*
4
5 2012; Wilke *et al.* 2012), given the similar buffering mineral assemblages in each of
6
7 the different lithologies the fluids may be of similar composition.
8
9

10 11 **Fluid Movements**

12
13
14 The zircon in the matrix shows abundant evidence of dissolution and this suggests
15
16 that fluid was pervasively present in the matrix whilst access more was restricted in
17
18 the clasts. Dissolution of altered zircon in the matrix, especially heterogeneous altered
19
20 zircon, results in preferential concentration of homogeneous altered zircon. The
21
22 dissolution of altered or metamict zircon will raise Zr contents in the fluid. This may
23
24 be synchronous with growth of new zircon lacking radiation damage or alteration that
25
26 will have lower solubility and so may precipitate as overgrowths from the same fluid.
27
28 A coupled dissolution-precipitation process may occur on the scale of single grains
29
30 (Geisler *et al.* 2007) or on a larger scale involving precipitation remote from the
31
32 zircon undergoing dissolution. Accurate mass balance associated with this
33
34 dissolution-reprecipitation process is impossible because of uncertainty surrounding
35
36 original abundance of zircon types in each host lithology. However the very small size
37
38 of overgrowths in comparison to the size of the host grains coupled to the significant
39
40 differences in zircon types in each lithology suggests that the dissolution and regrowth
41
42 of zircon is not a closed system. Overall fewer overgrowths are present than expected
43
44 from the potential volume of dissolution of heterogeneous zircon, and hence for
45
46 significant parts of the dissolution-regrowth history the scale of mobility exceeds the
47
48 scale of the sample. The distribution of overgrowths in the matrix is patchy and most
49
50 abundant within the mylonite zone. This implies that unless factors such as alkali/Al
51
52 ratios of fluids (Wilke *et al.* 2012) are of very local composition, zircon precipitation
53
54
55
56
57
58
59
60

1
2
3 is controlled by permeability contrasts within the matrix and hence overgrowth
4
5 distribution may define fluid pathways. Such pathways have been observed using the
6
7 distribution of microzircon, which may define zones of transient hydrofracturing in
8
9 greenschist facies metasedimentary rocks (Dempster & Chung 2013).
10
11 The zircon in granite and quartzite clasts both show similar overall levels of alteration
12
13 and so may be equally prone to fluid-related modification, however the styles of
14
15 alteration are different. Heterogeneous dark BSE altered zircon dominates the
16
17 population in the quartzite and appears to be typical of low grade metamorphic
18
19 settings (Hay & Dempster 2009a). This would be consistent with more open system
20
21 behaviour in the quartzite than within the granite clasts (Hay & Dempster 2009b).
22
23 Such behaviour may reflect the more pervasive fabric in the quartzite and importance
24
25 of deformation as a control on fluid access in the metamorphic realm. Zircon
26
27 alteration, dissolution and overgrowths are all strongly linked to the sparse muscovite
28
29 in the quartzite clasts. Quartz-mica boundaries may provide sites for preferential fluid
30
31 access due to anisotropic strain (Hippertt 1994). Chemically unaltered zircon is
32
33 typically isolated within quartz, and the presence of abundant porous zircon within the
34
35 quartzite clasts also suggests that there are many structural settings that have remained
36
37 isolated from fluids. The lack of spatial controls on the alteration process that are
38
39 linked to the margin of either clast type is striking (Fig. 8), hence fluid access does not
40
41 represent a diffusive infiltration controlled by proximity to the clast margins but is
42
43 linked to an irregular network of pathways. As such fluid access in the quartzite
44
45 appears to be channeled along foliation planes.
46
47
48
49
50

51
52 Despite the abundant petrographic evidence of sericitization of feldspar within the
53
54 granite clasts there is a lack of zircon overgrowths or evidence of dissolution and
55
56 hence limited redistribution of Zr. Homogeneous alteration of zircon is common
57
58
59
60

1
2
3 within the granite, suggesting that fluids are available on most grain boundaries but
4 that permeability is typically restricted. The dominance of homogeneous alteration of
5 zircon implies that scales of transport during dissolution-reprecipitation are very small
6 scale and hence that there is a lack of effective fluid pathways into these clasts,
7 perhaps equivalent to static fluid diffusion metasomatic processes (Korzhinskii 1970).
8 This interpretation is supported by evidence for “stalled” alteration within some zones
9 prone to alteration (Fig. 3A). Large feldspars in the granite may provide a rigid
10 framework (Tullis & Yund 1987), and limit penetrative deformation in these
11 greenschist facies rocks. The fact that less alteration occurs in zircon adjacent to
12 muscovite in the granite suggests that feldspar replacement reactions may limit
13 permeability (Moore *et al.* 1983) and hence zircon alteration. Such contrasts in
14 behaviour between zircon adjacent to muscovite in the granite and quartzite clasts also
15 point towards a dominant structural influence of the mineralogy rather than local
16 controls of fluid composition. Fluid consumption in the feldspar breakdown reaction
17 may act to generally reduce fluid availability within the granite. Although fine grained
18 alteration products do provide numerous grain boundaries and potential fluid
19 pathways, these are not preferentially utilized for subsequent fluid access associated
20 with zircon alteration. This suggests that active deformation is the key process
21 allowing fluid access rather than infiltration along grain boundaries and hence the
22 nature and abundance of those grain boundaries is not a crucial factor.
23
24
25
26
27
28
29
30
31
32
33
34
35
36
37
38
39
40
41
42
43
44
45
46
47
48

49 **DISCUSSION**

50 Fluids are increasingly recognized as important in all reactions and metamorphic
51 processes (Putnis & Austrheim, 2010), and this study has shown that their influence
52 crucially depends on deformation allowing fluids access to grain boundaries even
53
54
55
56
57
58
59
60

1
2
3 those lacking abundant fabric forming minerals. Other workers have shown that
4
5 porosity and permeability may be controlled by mineralogy (Arghe *et al.* 2011; Ferry
6
7 *et al.* 2013), and equilibrium wetting angles (Holness 1993; Price *et al.* 2004), but
8
9 there are many reports of a structural control of fluid pathways (e.g. Skelton *et al.*
10
11 1995; Abart *et al.* 2002; Pitcairn *et al.* 2010; Kleine *et al.* 2014). Zircon morphology
12
13 provides a sensitive monitor of fluid pathways in crustal rocks capable of recording a
14
15 range of different interactions.
16

17
18 Quartzite permeability is strongly controlled by active deformation creating transient
19
20 fluid pathways. Creep cavitation (Fusseis *et al.* 2009) provides a mechanism for
21
22 driving fluids along grain boundaries of deforming clasts. The transient permeability
23
24 of quartzite suggests that few lithologies are impermeable during deformation,
25
26 although this will be constrained by the conditions that control the structural response.
27
28 Hence permeability is restricted in granite by a combination of the strength of the
29
30 feldspar dominated structural framework in the greenschist facies conditions together
31
32 with feldspar-breakdown, water-consuming reactions that reduce porosity and create
33
34 an apparent barrier to fluid movement. However the granite may have a more
35
36 permeable response at higher temperatures (Rosenberg & Stünitz 2003). Muscovite
37
38 presence appears to act as a general barrier to fluid flow in the granite, but during
39
40 penetrative deformation it enhances fluid access in the quartzite. The response of
41
42 minerals to deformation is an important factor in allowing fluid access and it appears
43
44 that phyllosilicates are primary influences in controlling metamorphic equilibration
45
46 (Dempster & Tanner 1997) from both a structural and chemical perspective.
47
48 Permeability will reflect a complex interplay between fluid consumption and
49
50 generation, and the differential response of lithologies to deformation.
51
52
53
54
55
56
57
58
59
60

ACKNOWLEDGEMENTS

This research was supported by the University of Glasgow. Peter Chung and John Gilleece are thanked for technical support. Alasdair Skelton and Bruce Yardley are thanked for their thoughtful reviews of the manuscript.

REFERENCES

- Abart R, Badertscher N, Burkhard M & Povoden E (2002) Oxygen, carbon and strontium isotope systematics in two profiles across the Glarus thrust: implications for fluid flow. *Contributions to Mineralogy and Petrology*, **143**, 192-208.
- Arghe F, Skelton A & Pitcairn I (2011) Spatial coupling between spilitization and carbonation of basaltic sills in SW Scottish Highlands: evidence of a mineralogical control of metamorphic fluid flow. *Geofluids* **11**, 245-259.
- Ayers JC & Watson EB (1991) Solubility of apatite, monazite, zircon, and rutile in supercritical aqueous fluids with implications for subduction zone geochemistry. *Philosophical Transactions of the Royal Society of London (A)*, **335**, 365-375
- Ayers JC, Zhang L, Luo, Y & Peters TJ (2012) Zircon solubility in alkaline aqueous fluids at upper crustal conditions. *Geochimica et Cosmochimica Acta*, **96**, 18-28.
- Bickle MJ & McKenzie DP (1987) The transport of heat and matter by fluids during metamorphism. *Contributions to Mineralogy and Petrology*, **95**, 384-392.
- Cartwright I (1997) Permeability generation and resetting of tracers during metamorphic fluid flow: implications for advective-dispersion models. *Contributions to Mineralogy and Petrology* **129**, 198-208.
- Chamberlain CP & Rumble D (1988) Thermal anomalies in a regional metamorphic terrane: an isotopic study of the role of fluids. *Journal of Petrology*, **29**, 1215-1232.

- 1
2
3 Crowley QG & Strachan RA (2015) U-Pb zircon constraints on obduction initiation of
4
5 the Unst Ophiolite: and oceanic core complex in the Scottish Caledonides?
6
7 *Journal of the Geological Society, London*, **172**, 279-282.
8
9
10 Delattre S, Utsunomiya S, Ewing RC, Boeglin J-L, Braun J-J, Balan E & Calas G
11
12 (2007) Dissolution of radiation-damaged zircon in lateritic soils. *American*
13
14 *Mineralogist*, **92**, 1978-1989.
15
16 Dempster TJ, Campanile D & Holness MB (2006) Imprinted textures on apatite: a
17
18 guide to paleoporosity and metamorphic recrystallisation. *Geology*, **34**, 897-900.
19
20 Dempster TJ & Chung P (2013) Metamorphic zircon: tracking fluid pathways and the
21
22 implications for the preservation of detrital zircon. *Journal of the Geological*
23
24 *Society*, **170**, 631-639.
25
26
27 Dempster TJ, Hay DC & Bluck BJ (2004) Zircon growth in slate. *Geology*, **32**, 221-
28
29 224.
30
31
32 Dempster TJ, Hay DC, Gordon SH & Kelly NM (2008a) Micro-zircon: origin and
33
34 evolution during metamorphism. *Journal of Metamorphic Geology*, **26**, 499-507.
35
36
37 Dempster TJ, Martin JC & Shipton ZK (2008b) Zircon dissolution in a ductile shear
38
39 zone, Monte Rosa granite gneiss, northern Italy. *Mineralogical Magazine*, **74**,
40
41 971-986.
42
43
44 Dempster TJ & Tanner PWG (1997) The biotite isograd, Central Pyrenees: a
45
46 deformation - controlled reaction. *Journal of Metamorphic Geology*, **15**, 531-54
47
48
49 Ewing RC, Haaker RF & Lutze W (1982) Leachability of zircon as a function of
50
51 alpha dose. In: Lutze W (ed) Scientific basis for radioactive waste management V,
52
53 Elsevier, Amsterdam, pp 3899-397.
54
55
56 Ferry JM (1984) A biotite isograd in south-central Maine, U.S.A.: mineral reactions,
57
58 fluid transfer, and heat transfer. *Journal of Petrology*, **25**, 871-893.
59
60

- 1
2
3 Ferry JM, Winslow NW & Penniston-Dorland SC (2013) Re-evaluation of
4
5 infiltration-driven regional metamorphism in northern New England: New
6
7 transport models with solid solution and cross-layer equilibration of fluid
8
9 composition. *Journal of Petrology*, **54**, 2455-2485
10
11
12 Flinn D (1956) On the deformation of the Funzie conglomerate, Fetlar, Shetland.
13
14 *Journal of Geology*, **64**, 480-505.
15
16 Flinn, D. & Oglethorpe, R.J.D. (2005) A history of the Shetland Ophiolite Complex.
17
18 *Scottish Journal of Geology*, **41**, 141-148.
19
20
21 Fusses F, Regenauer-Lieb K, Liu J, Hough RM & De Carlo F (2009) Creep
22
23 cavitation can establish a dynamic granular fluid pump in ductile shear zones.
24
25 *Nature*, **459**, 974-977
26
27
28 Geisler T, Pidgeon RT, Kurtz R, van Bronswijk W & Schleicher H (2003)
29
30 Experimental hydrothermal alteration of partially metamict zircon. *American*
31
32 *Mineralogist*, **88**, 1496- 1513.
33
34
35 Geisler T, Schaltegger U. & Tomaschek F (2007) Re-equilibration of zircon in
36
37 aqueous fluids and melts. *Elements*, **3**, 43-50.
38
39
40 Geisler T, Seydoux-Guillaume A-M, Wiedenbeck M, Wirth R, Berndt J, Zhang M,
41
42 Milhailova B, Putnis A, Salje EKH & Schlüter J (2004) Periodic precipitation
43
44 pattern formation in hydrothermally treated metamict zircon. *American*
45
46 *Mineralogist*, **89**, 1341-1347.
47
48
49 Harley SL & Kelly NM (2007) Zircon tiny but timely. *Elements*, **3**, 13-18.
50
51
52 Hay DC & Dempster TJ (2009a) Zircon behaviour during low temperature
53
54 metamorphism. *Journal of Petrology*, **50**, 571-589.
55
56
57 Hay DC & Dempster TJ (2009b) Zircon alteration, formation and preservation in
58
59 sandstones. *Sedimentology*, **56**, 2175-2191.
60

- 1
2
3 Hippertt JFM (1994) Grain boundary microstructures in micaceous quartzite:
4
5 Significance for fluid movement and deformation processes in low metamorphic
6
7 grade shear zones. *Journal of Geology*, **102**, 331-348.
8
9
10 Holness MB (1993) Temperature and pressure dependence of quartz-aqueous fluid
11
12 dihedral angles: the control of adsorbed H₂O on the permeability of quartzites.
13
14 *Earth and Planetary Science Letters*, **117**, 363-377.
15
16 Holness MB & Watt GR (2001) Quartz recrystallisation and fluid flow during contact
17
18 metamorphism: A cathodoluminescence study. *Geofluids*, **1**, 215-228.
19
20
21 Kleine BI, Skelton ADL, Huet B & Pitcairn IK (2014) Preservation of Blueschist-
22
23 facies Minerals along a Shear Zone by Coupled Metasomatism and Fast-flowing
24
25 CO₂- bearing Fluids. *Journal of Petrology*, **55**, 1905-1939.
26
27
28 Kohn MJ & Valley JW (1994) Oxygen isotope constraints on metamorphic fluid flow,
29
30 Townshend Dam, Vermont, USA. *Geochimica et Cosmochimica Acta*, **58**, 5551-
31
32 5568.
33
34 Korzhinskii DS (1970) Theory of metasomatic zoning. Oxford University Press,
35
36 Oxford.
37
38
39 Kröner A (2010) The role of geochronology in understanding continental evolution.
40
41 *Geological Society, London, Special Publication*, **338**, 179-196.
42
43 Lee JKW & Tromp J (1995) Self-Induced fracture generation in zircon. *Journal of*
44
45 *Geophysical Research-Solid Earth*, **100**, 17753-17770.
46
47
48 Moore DE, Morrow CA & Byerlee JD (1983) Chemical reactions accompanying fluid
49
50 flow through granite held in a temperature gradient. *Geochimica et Cosmochimica*
51
52 *Acta*, **47**, 445-453.
53
54
55
56
57
58
59
60

- 1
2
3 Oliver NHS & Bons PD (2001) Mechanisms of fluid flow and fluid-rock interactions
4
5 in fossil metamorphic hydrothermal systems inferred from vein-wallrock patterns,
6
7 geometry and microstructure. *Geofluids*, **1**, 137-162.
8
9
10 Pitcairn IK, Skelton ADL, Broman C, Arghe F & Boyce A (2010) Structurally
11
12 focused fluid flow during orogenesis: the Islay Anticline, SW Highlands,
13
14 Scotland. *Journal of the Geological Society, London*, **167**, 659-674.
15
16
17 Price JD, Wark DA, & Watson BE (2004) Grain-scale permeabilities of synthetic
18
19 quartzite with volumetrically minor phlogopite, corundum, or aluminosilicate.
20
21 *Earth and Planetary Science Letters*, **227**, 491-504.
22
23
24 Putnis A & Austrheim H (2010) Fluid - induced processes: metasomatism and
25
26 metamorphism. *Geofluids*, **10**, 254-269
27
28
29 Rasmussen B (2005) Zircon growth in very low grade metasedimentary rocks:
30
31 evidence for zirconium mobility at similar to 250°C. *Contributions to Mineralogy
32
33 and Petrology* 150, 146-155.
34
35
36 Rayner N, Stern RA & Carr D (2005) Grain-scale variations in trace element
37
38 composition of fluid-altered zircon, Acasta Gneiss Complex, northwestern
39
40 Canada. *Contributions to Mineralogy and Petrology*, **148**, 721-734.
41
42
43 Rosenberg CL & Stünitz H (2003) Deformation and recrystallization of plagioclase
44
45 along a temperature gradient: an example from the Bergell tonalite. *Journal of
46
47 Structural Geology*, **25**, 389-408.
48
49
50 Skelton ADL, Graham CM & Bickle MJ (1995) Lithological and structural controls
51
52 on regional 3-D fluid flow patterns during greenschist facies metamorphism of the
53
54 Dalradian of the SW Scottish Highlands. *Journal of Petrology*, **36**, 563-586.
55
56
57 Tullis J & Yund RA (1987) Transition from cataclastic flow to dislocation creep of
58
59 feldspar: mechanisms and microstructures. *Geology*, **15**, 606-609.
60

1
2
3 Wilde SA, Valley JW, Peck WH & Graham CM (2001) Evidence from detrital
4
5 zircons for the existence of continental crust and ocean on the Earth 4.4 Gyr ago.
6
7 *Nature*, **409**, 175-177.

8
9
10 Wilke M, Schmidt C, Dubraille J, Appel K, Borchert M, Kvashnina K & Manning CE
11
12 (2012) Zircon solubility and zirconium complexation in $\text{H}_2\text{O} + \text{Na}_2\text{O} + \text{SiO}_2 \pm$
13
14 Al_2O_3 fluids at high pressure and temperature. *Earth and Planetary Science*
15
16 *Letters*, **349**, 15-25.

17
18
19 Yardley BWD (2009) The role of water in the evolution of the continental crust.
20
21 *Journal of the Geological Society, London*, **166**, 585-600.

22 23 24 25 **FIGURE CAPTIONS**

26
27 **Fig. 1.** Field photograph of the Fetlar metaconglomerate. Aligned flattened and
28
29 elongated clasts in phyllitic matrix. Hammer head is 12cm long.

30
31
32
33
34 **Fig. 2.** Photomicrographs in crossed polarized light. (A) Quartzite clast in matrix
35
36 (FZ88.1.2) showing clast matrix boundary with strong fabric in matrix and quartz-rich
37
38 matrix to the right of the clast in a pressure shadow like zone; (B) Interior of quartzite
39
40 clast (FZ88.1.1) showing fabric and sparse muscovite with high interference colours
41
42 and sutured boundaries of quartz; (C) Quartzite matrix boundary (FZ88.4) showing
43
44 alignment of within quartzite and fine grained muscovite-rich matrix; (D) Matrix area
45
46 (FZ88.4) showing fine grained dark mylonite band in upper right hand area within
47
48 aligned quartz-rich area of matrix; (E) Muscovite-rich matrix area (FZ88.4) showing
49
50 large deformed muscovite with fine grained aligned muscovite and quartz and
51
52 plagioclase porphyroclasts; (F) Contact between muscovite- and biotite-rich matrix
53
54
55
56 (lower right) and altered granite clast (FZ89.4.1) in which plagioclase has been
57
58
59
60

1
2
3 largely altered to fine grained muscovite. Original quartz has recrystallized to fine
4
5 grainsize; (G) Largely unaltered central part of granite clast (FZ89.4.2) containing
6
7 large plagioclase grains in finer recrystallised matrix; (H) Partially altered granite
8
9 from centre of clast (FZ89.4.2) showing muscovite alteration along edges of
10
11 plagioclase and adjacent recrystallized quartz.
12
13

14
15
16 **Fig. 3.** Representative backscattered electron (BSE) images of zircons from clasts (A-
17
18 B: Granite clast; C-H: Quartzite clast). (A) Homogeneous alteration along growth
19
20 zones with bulbous patchy alteration in core areas; (B) Homogeneous alteration along
21
22 growth zones with minor dissolution on right edge; (C) Largely unaltered core with
23
24 large zircon overgrowth; (D) Heterogeneous altered zircon with xenotime
25
26 overgrowths; (E) Small unaltered euhedral zircon; (F) Homogeneous alteration of
27
28 growth zones in the core area with larger area of heterogeneous alteration in
29
30 surrounding area; (G) Porous zircon with patches of heterogeneous alteration; (H)
31
32 Porous chemically unmodified zircon.
33
34
35
36
37
38

39 **Fig. 4.** Representative backscattered electron (BSE) images of zircons from matrix.
40
41 (A) Homogeneous alteration of internal growth zones; (B) Patchy homogeneous
42
43 alteration of core area with radial cracking of rim allowing fluid access; (C) Extensive
44
45 homogeneous alteration; (D) Small unaltered euhedral zircon; (E) Porous zircon with
46
47 large overgrowths; (F) Fractured zircon with lack of small angular fragments; (G)
48
49 Largely unaltered zircon with overgrowths; (H) Heterogeneous alteration of zircon
50
51 with evidence of dissolution (rounding of fragments) and dispersal parallel to rock
52
53 cleavage; (I) Heterogeneous alteration with large embayments associated with
54
55 dissolution and replacement by quartz; (J) Homogeneous alteration with evidence of
56
57
58
59
60

1
2
3 deformation and dissolution.
4
5
6

7 **Fig. 5.** Histogram showing the proportion of zircons with overgrowths in each
8 lithology.
9
10

11
12
13 **Fig. 6.** Histogram showing the amount of alteration of zircon in different host
14 lithologies.
15
16
17

18
19
20 **Fig. 7.** Histogram showing the proportions of different altered zircon types within
21 each lithology.
22
23
24

25
26
27 **Fig. 8.** Plots showing relationship between the amount of alteration in individual
28 zircon grains and their proximity to the clast margin for A. Quartzite clasts and B.
29 Granite clasts.
30
31
32

33
34
35 **Fig. 9.** Histograms showing the influence of adjacent mineralogy on A. the area of
36 alteration in the zircon and B. the area of overgrowth around the zircon.
37
38
39
40
41
42
43
44
45
46
47
48
49
50
51
52
53
54
55
56
57
58
59
60



Fig. 1. Field photograph of the Fetlar metaconglomerate. Aligned flattened and elongated clasts in phyllitic matrix. Hammer head is 12cm long.
209x296mm (150 x 150 DPI)

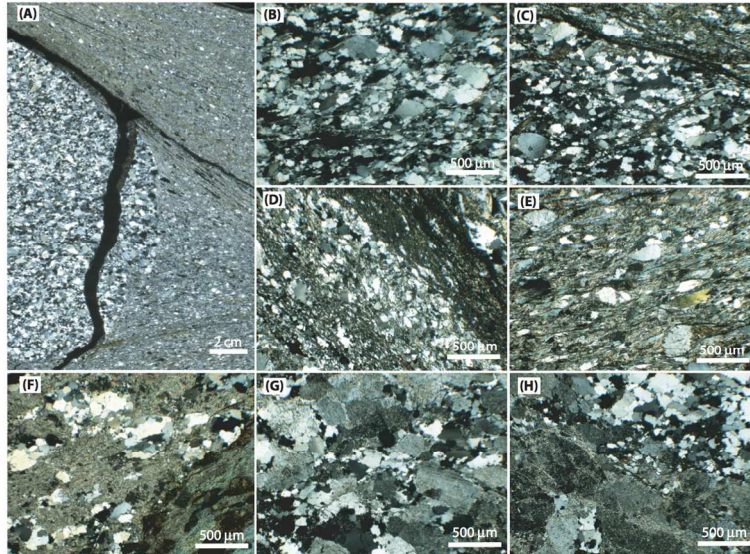


Fig. 2. Photomicrographs in crossed polarized light. (A) Quartzite clast in matrix (FZ88.1.2) showing clast matrix boundary with strong fabric in matrix and quartz-rich matrix to the right of the clast in a pressure shadow like zone; (B) Interior of quartzite clast (FZ88.1.1) showing fabric and sparse muscovite with high interference colours and sutured boundaries of quartz; (C) Quartzite matrix boundary (FZ88.4) showing alignment of within quartzite and fine grained muscovite-rich matrix; (D) Matrix area (FZ88.4) showing fine grained dark mylonite band in upper right hand area within aligned quartz-rich area of matrix; (E) Muscovite-rich matrix area (FZ88.4) showing large deformed muscovite with fine grained aligned muscovite and quartz and plagioclase porphyroclasts; (F) Contact between muscovite- and biotite-rich matrix (lower right) and altered granite clast (FZ89.4.1) in which plagioclase has been largely altered to fine grained muscovite. Original quartz has recrystallized to fine grainsize; (G) Largely unaltered central part of granite clast (FZ89.4.2) containing large plagioclase grains in finer recrystallised matrix; (H) Partially altered granite from centre of clast (FZ89.4.2) showing muscovite alteration along edges of plagioclase and adjacent recrystallized quartz.

296x247mm (150 x 150 DPI)

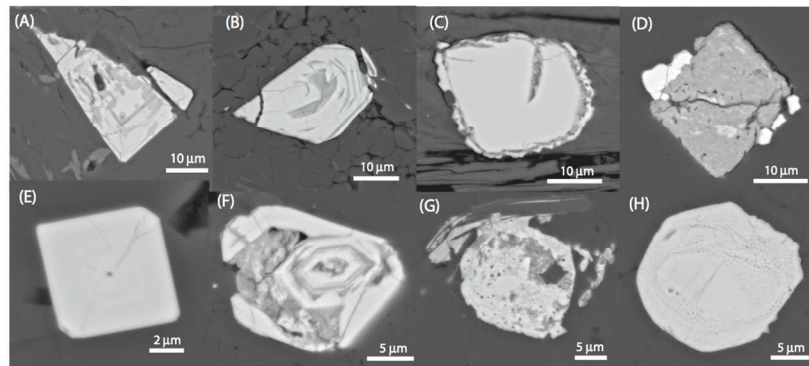


Fig. 3. Representative backscattered electron (BSE) images of zircons from clasts (A-B: Granite clast; C-H: Quartzite clast). (A) Homogeneous alteration along growth zones with bulbous patchy alteration in core areas; (B) Homogeneous alteration along growth zones with minor dissolution on right edge; (C) Largely unaltered core with large zircon overgrowth; (D) Heterogeneous altered zircon with xenotime overgrowths; (E) Small unaltered euhedral zircon; (F) Homogeneous alteration of growth zones in the core area with larger area of heterogeneous alteration in surrounding area; (G) Porous zircon with patches of heterogeneous alteration; (H) Porous chemically unmodified zircon.
217x296mm (150 x 150 DPI)

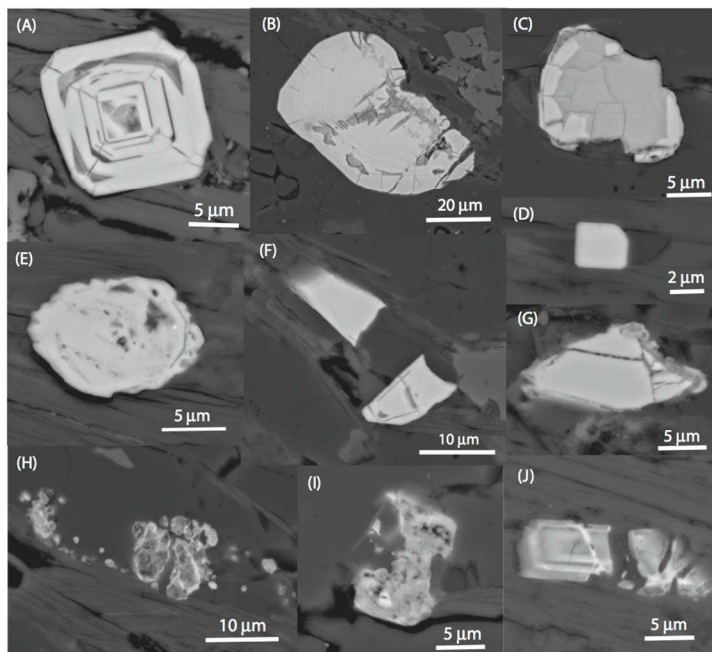


Fig. 4. Representative backscattered electron (BSE) images of zircons from matrix. (A) Homogeneous alteration of internal growth zones; (B) Patchy homogeneous alteration of core area with radial cracking of rim allowing fluid access; (C) Extensive homogeneous alteration; (D) Small unaltered euhedral zircon; (E) Porous zircon with large overgrowths; (F) Fractured zircon with lack of small angular fragments; (G) Largely unaltered zircon with overgrowths; (H) Heterogeneous alteration of zircon with evidence of dissolution (rounding of fragments) and dispersal parallel to rock cleavage; (I) Heterogeneous alteration with large embayments associated with dissolution and replacement by quartz; (J) Homogeneous alteration with evidence of deformation and dissolution.

209x296mm (150 x 150 DPI)

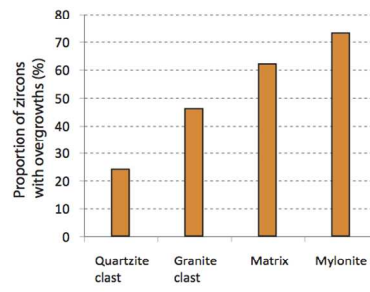


Fig. 5. Histogram showing the proportion of zircons with overgrowths in each lithology.
209x296mm (150 x 150 DPI)

1
2
3
4
5
6
7
8
9
10
11
12
13
14
15
16
17
18
19
20
21
22
23
24
25
26
27
28
29
30
31
32
33
34
35
36
37
38
39
40
41
42
43
44
45
46
47
48
49
50
51
52
53
54
55
56
57
58
59
60

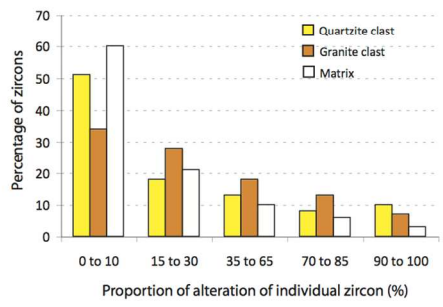


Fig. 6. Histogram showing the amount of alteration of zircon in different host lithologies.
209x296mm (150 x 150 DPI)

1
2
3
4
5
6
7
8
9
10
11
12
13
14
15
16
17
18
19
20
21
22
23
24
25
26
27
28
29
30
31
32
33
34
35
36
37
38
39
40
41
42
43
44
45
46
47
48
49
50
51
52
53
54
55
56
57
58
59
60

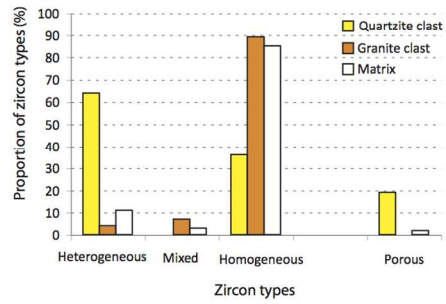


Fig. 7. Histogram showing the proportions of different altered zircon types within each lithology.
209x296mm (150 x 150 DPI)

1
2
3
4
5
6
7
8
9
10
11
12
13
14
15
16
17
18
19
20
21
22
23
24
25
26
27
28
29
30
31
32
33
34
35
36
37
38
39
40
41
42
43
44
45
46
47
48
49
50
51
52
53
54
55
56
57
58
59
60

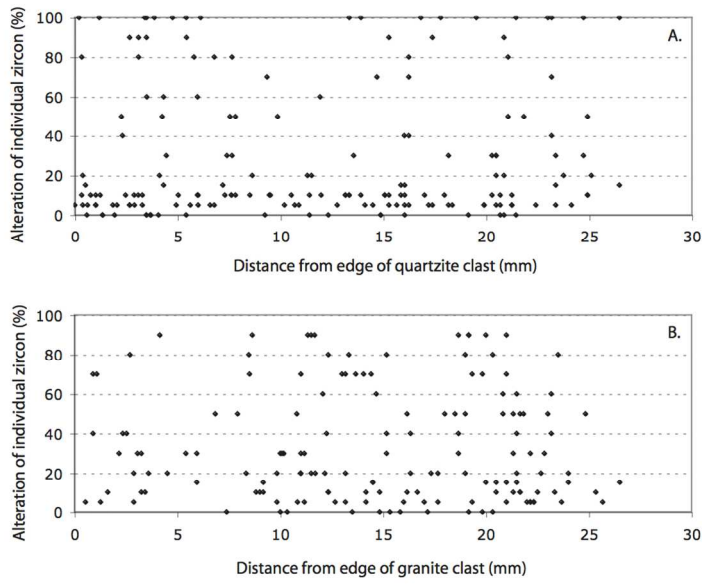


Fig. 8. Plots showing relationship between the amount of alteration in individual zircon grains and their proximity to the clast margin for A. Quartzite clasts and B. Granite clasts.
209x296mm (150 x 150 DPI)

1
2
3
4
5
6
7
8
9
10
11
12
13
14
15
16
17
18
19
20
21
22
23
24
25
26
27
28
29
30
31
32
33
34
35
36
37
38
39
40
41
42
43
44
45
46
47
48
49
50
51
52
53
54
55
56
57
58
59
60

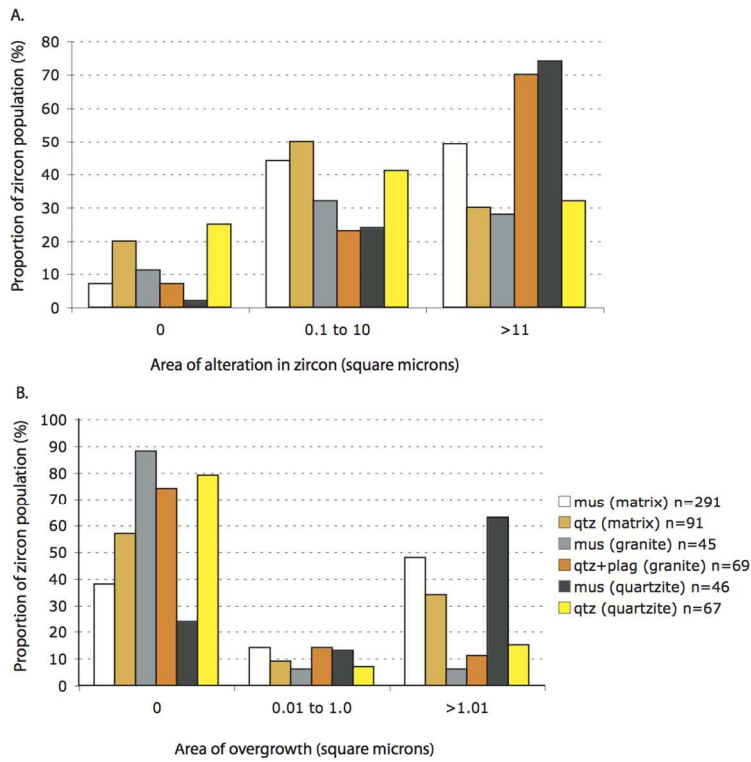


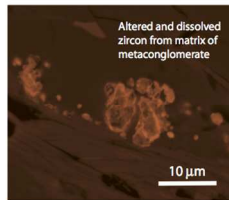
Fig. 9. Histograms showing the influence of adjacent mineralogy on A. the area of alteration in the zircon and B. the area of overgrowth around the zircon.
209x296mm (150 x 150 DPI)

1
2
3 **Controls on fluid movement in crustal lithologies: evidence from zircon in**
4
5 **metaconglomerates from Shetland**
6

7 Tim Dempster*, Fiona Macdonald
8

9
10 Movement of low temperature fluids through rocks causes alteration of zircon
11
12 resulting in chemical modification, dissolution and new growth. This investigation of
13
14 zircon textures in different clast types and matrix in a metamorphosed conglomerate
15
16 reveals different responses of zircon linked to different permeability controls. Fluid
17
18 influx in these metamorphic rocks is shown to primarily occur along discrete
19
20 pathways controlled by the response of quartz, plagioclase and phyllosilicates to
21
22 deformation.
23
24
25
26
27
28
29
30
31
32
33
34
35
36
37
38
39
40
41
42
43
44
45
46
47
48
49
50
51
52
53
54
55
56
57
58
59
60

1
2
3
4
5
6
7
8
9
10
11
12
13
14
15
16
17
18
19
20
21
22
23
24
25
26
27
28
29
30
31
32
33
34
35
36
37
38
39
40
41
42
43
44
45
46
47
48
49
50
51
52
53
54
55
56
57
58
59
60



Backscattered electron image of altered zircon
209x296mm (150 x 150 DPI)